

# Omega Currents in Voltage-Gated Ion Channels: What Can We Learn from Uncovering the Voltage-Sensing Mechanism Using MD Simulations?

MOUNIR TAREK\* AND LUCIE DELEMOTTE†

*Université de Lorraine, Equipe Théorie-Modélisation-Simulations,  
SRSMC, UMR 7565, Vandoeuvre les Nancy, France, and CNRS, Equipe  
Théorie-Modélisation-Simulations, UMR 7565, Vandoeuvre les Nancy, France*

RECEIVED ON OCTOBER 15, 2012

## CONSPECTUS

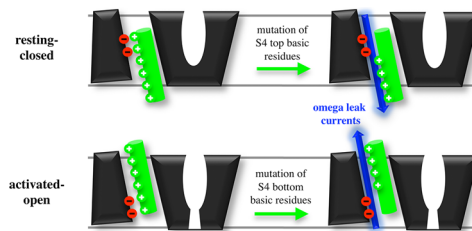
**I**on channels conduct charged species through otherwise impermeable biological membranes. Their activity supports a number of physiological processes, and genetic mutations can disrupt their function dramatically. Among these channels, voltage gated cation channels (VGCCs) are ubiquitous transmembrane proteins involved in electrical signaling. In addition to their selectivity for ions, their function requires membrane-polarization-dependent gating.

Triggered by changes in the transmembrane voltage, the activation and deactivation of VGCCs proceed through a sensing mechanism that prompts motion of conserved positively charged (basic) residues within the S4 helix of a four-helix bundle, the voltage sensor domain (VSD). Decades of experimental investigations, using electrophysiology, molecular biology, pharmacology, and spectroscopy, have revealed details about the function of VGCCs. However, in 2005, the resolution of the crystal structure of the activated state of one member of the mammalian voltage gated potassium (Kv) channels family (the Kv1.2) enabled researchers to make significant progress in understanding the structure–function relationship in these proteins on a molecular level. In this Account, we review the use of a complementary technique, molecular dynamics (MD) simulations, that has offered new insights on this timely issue.

Starting from the “open-activated state” crystal structure, we have carried out large-scale all atom MD simulations of the Kv1.2 channel embedded in its lipidic environment and submitted to a hyperpolarizing (negative) transmembrane potential. We then used steered MD simulations to complete the full transition to the resting-closed state. Using these procedures, we have followed the operation of the VSDs and uncovered three intermediate states between their activated and deactivated conformations. Each conformational state is characterized by its network of salt bridges and by the occupation of the gating charge transfer center by a specific S4 basic residue. Overall, the global deactivation mechanism that we have uncovered agrees with proposed kinetic models and recent experimental results that point towards the presence of several intermediate states.

The understanding of these conformations has allowed us to examine how mutations of the S4 basic residues analogous to those involved in genetic diseases affect the function of VGCCs. In agreement with electrophysiology experiments, mutations perturb the VSD structure and trigger the appearance of state-dependent “leak” currents. The simulation results unveil the key elementary molecular processes involved in these so-called “omega” currents. We generalize these observations to other members of the VGCC family, indicating which type of residues may generate such currents and which conditions might cause leaks that prevent proper function of the channel.

Today, the understanding of the intermediate state conformations enables researchers to confidently tackle other key questions such as the mode of action of toxins or modulation of channel function by lipids.



## Introduction

First discovered in the early 1950s, *excitable cells* are crucial for the function of superior organisms: they respond to electric voltage pulses by giving rise to currents across their

plasma membrane. Twenty years later, transmembrane proteins, called *voltage-gated cation channels (VGCCs)*, were identified as the molecular level components that account for the voltage-dependent conduction across excitable

cell membranes. Such pores switch from a closed to open state when the transmembrane potential is made more positive than the cell resting potential (depolarization).<sup>1</sup> These channels are ubiquitous to excitable cells, that is, are found in the heart, in the nervous system, and in many other organs. They fulfill a wide variety of biological functions and are therefore sensitive to a large number of modulating factors, for example, action of drugs or anesthetics, alteration of the membrane lipids embedding them, and so forth. Similarly, mutations of these channels can give rise to familial genetic diseases, called channelopathies.<sup>2</sup>

With the advent of voltage clamp techniques, electrophysiology experiments allowed the discovery in the 1970s of a characteristic feature of VGCCs: during activation (transition from closed (resting) to open (activated) state), they produce small transient currents, named gating currents.<sup>3</sup> Their integral is called the *gating charge* and measures the quantity of charge transported by the channel during activation. In the 1980s, sequencing the first VGCCs revealed a trimeric assembly of six transmembrane helices. The fold and assembly of the two N-terminal helices (S5 and S6) form the pore, the domain that is responsible for the selectivity and transport of ions across the membrane. The other four (S1–S4) constitute voltage sensor domains (VSD), responsible for sensing the transmembrane voltage changes. The fourth transmembrane helical segment (S4) contains four to seven of positively charged, basic, residues (mostly arginines) that sense and respond to the local electric field. These residues trigger the appearance of the gating currents. During activation of *Shaker*, the first potassium VGCC (Kv) channel identified, for example, the S4 basic residues transport ~12–14 elementary charges across the membrane.<sup>4,5</sup>

The kinetics of the ionic (G) and gating (Q) currents signal a multistep process, involving one or more intermediate states. The conformational transitions between states within each VSD are independent, and only the last intermediate to open transition is concerted.<sup>6,7</sup> all VSDs need to be activated to open the pore.<sup>8</sup> Early models, as the Zagotta–Hoshi–Aldrich model have considered three VSD states.<sup>6</sup> Others, involving measurements over a broader voltage range, involve additional states. More recent models propose four to five states.<sup>9–12</sup>

The gating charge is a fundamental property that not only determines the voltage dependency of channel activation, but also constraints the physical models of VSD operation. To describe the latter, three main models have been set forth. In the *helical screw model*, S4 moves independently from the rest of the voltage sensor domain in a screwlike

motion, translating by ~10–20 Å while rotating about its own axis by 180°. <sup>13,14</sup> In this scheme, supported by mutagenesis studies, several salt bridges between S4 arginines and negatively charged residues of S1–S3 are broken/formed when S4 moves in response to the electric field changes.<sup>15</sup> The *transporter model* involves instead a large reorganization of the local electrostatic potential with a S4 vertical translation limited to a few Å. This assumption derives mainly from fluorescence measurements.<sup>16</sup> The *paddle model* involves the complete translation of the S3–S4 paddle across the bilayer and has been abandoned in the light of new results.<sup>17</sup> Recently, a large number of studies have sought to conciliate these models, and a unified picture has emerged in the last years: the transmembrane translation of S4 is of intermediate magnitude and the VSD salt bridges rearrangement is decisive for channel function.<sup>18</sup>

The biggest advance in understanding the molecular mechanism of VGCCs comes probably from the resolution of the first mammalian potassium channel crystal structure, the *Kv1.2*.<sup>19</sup> In this structure, the pore was captured in the open state and the VSDs in their activated conformation (S4 “up”). This structure, overall consistent with a large number of previous electrophysiology measurements, has confirmed or revealed molecular details, such as the salt bridge network involved in the activated state of the VSD or the interaction of lipid head groups with the top basic residues of S4.

However outstanding the progress achieved thanks to exquisite quantitative electrophysiology experiments and the breakthrough achievements mentioned above, questions about the molecular mechanism of VSD deactivation and the topology of the *Kv1.2* intermediate and resting states remain unanswered. Evidently, insight into such a mechanism will enable one to tackle challenging issues such as the molecular implication of the modulation of the function of such channels by drugs, toxins or the effect of genetic mutations.

Several groups have provided answers to this crucial question of the topology of the resting state by building closed state models of *Kv1.2* by homology and de novo modeling (Rosetta-membrane) using a plethora of experimentally defined constraints<sup>20–22</sup> and subsequently equilibrating them using MD simulations.<sup>23,24</sup> We, on the other hand, have chosen a complementary strategy: seeking to uncover also the molecular structure of intermediate states of the VSD, we have used MD simulations to follow the channel response to hyperpolarized (negative) transmembrane potentials.<sup>25</sup>

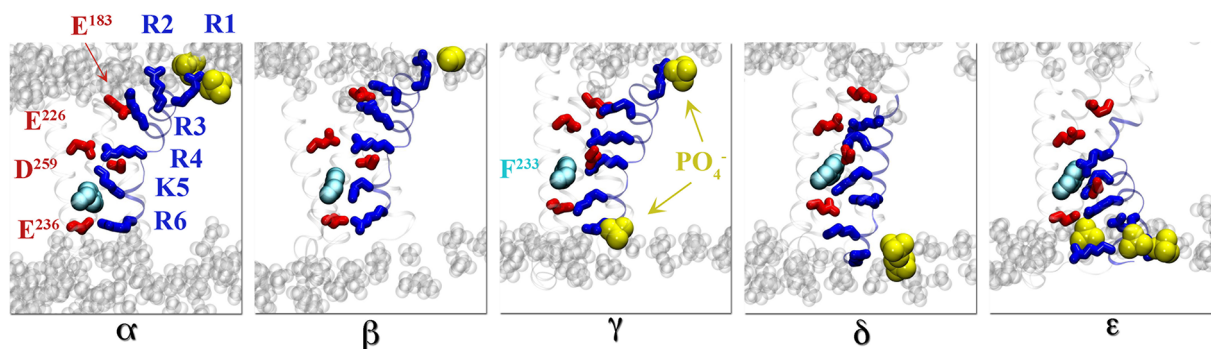


**FIGURE 1.** Molecular views of the VSDs in the five key conformations, obtained from the crystal structure ( $\alpha$ ), using MD simulations under an hyperpolarized voltage ( $\beta$  and  $\gamma$ ) and a steered MD protocol ( $\delta$  and  $\epsilon$ ). The side-view highlights the state-dependent position of the S4 basic residues (blue sticks) and the salt bridges they form with the acidic residues (red sticks) of the other VSD segments or with the lipid headgroup  $\text{PO}_4^-$  moieties (yellow). The highly conserved residue  $\text{F}^{233}$  of S2 is shown as cyan spheres. Copyright 2011 from PNAS.

## Deactivation of Kv1.2

We followed the deactivation of the full length Kv1.2 embedded in a lipid bilayer by hyperpolarizing the membrane. Previous simulations imposed an hyperpolarizing transmembrane potential ( $\Delta V$ ) by applying an external electric field,<sup>26–28</sup> a method that enables one to measure directly gating currents in the form of protein charge displacement across the membrane.<sup>23,29,30</sup> Here, in contrast, we create a charge imbalance between both sides of the membrane. To prevent communication between them through periodic boundary conditions, we introduce a vacuum slab between periodic images in the  $z$  direction.<sup>31</sup> This method is a modified version of the double bilayer setup,<sup>32</sup> that avoids asymmetry and overcost. It also enables to record directly the charge  $Q(t)$  that is transported across the membrane capacitor,<sup>30,33</sup> that is, the gating charge routinely measured in electrophysiology. In such a setup, reorganization of charges across the membrane leads to a drop of  $\Delta V$  and we can trace back conformational changes of the channel that produce a measurable gating charge to a change in  $\Delta V$ .

We have generated an  $>2 \mu\text{s}$  trajectory of the Kv1.2/membrane system subject to a large hyperpolarized  $\Delta V$ . Due to the limited time scale we could reach, we have submitted the system to  $\Delta V \sim -600 \text{ mV}$ , a transmembrane voltage  $\sim 10$  times higher than in experiments, to speed up the response of the channel. We have monitored the stability of the Kv1.2 channel and of the membrane along the simulation to ensure that such a high transmembrane voltage does not destabilize the system.  $Q(t)$  recorded along the MD simulation underwent several drops, indicating a significant channel electrical activity. We linked the  $Q(t)$  drops to conformational rearrangements within the VSD: the positive charges of S4 (R294, R297, R300, R303, K306, and R309, called hereafter R1 to R6) shifted down stepwise from

external (top) to internal (bottom) negatively charge binding sites in a ratchetlike motion. These binding sites are acidic amino-acids of segments S1–S3 (E183, E226, D259, and E236) and  $\text{PO}_4^-$  groups of the lipid headgroups of the outer and inner bilayer leaflets (Figure 1). Along our simulation, all subunits underwent a first conformational rearrangement toward a stable conformation named  $\beta$ . One subunit underwent a second rearrangement, reaching another downstream conformation  $\gamma$ . Note that this observation agrees with experiments suggesting that most conformational transitions of the four VSDs of the channel are independent, with only the last intermediate to open transition being a concerted process.<sup>8</sup>

Such a brute force simulation, limited to a short time scale, was not long enough to bring the channel to its resting state. We therefore designed a steered MD protocol to propagate this ratchetlike motion: the positive residues of S4 in all VSDs were pulled simultaneously downward toward the next binding site (countercharge). Two additional conformations of the VSD  $\delta$  and  $\epsilon$  were hence obtained.

The  $\epsilon$  conformation was found to be consistent with many constraints to the resting state derived from electrophysiology experiments. First, the gating charge measured during the transition from  $\alpha$  to  $\epsilon \sim 12.8 \pm 0.3e$  agrees with values obtained for *Shaker*-like channels.<sup>4,5</sup> Next, measured distances of residue pairs within the resting state VSDs comply with interactions that were probed under hyperpolarized voltages by electrostatic interactions or disulfide bridges approaches.<sup>25</sup> Finally, we checked further the positions of S4 basic residues in  $\epsilon$  by probing the effect of mutations of the top R1 and R2 arginines (see next paragraph).<sup>34</sup>

Interestingly, despite the use of a nonphysiological transmembrane voltage, the complete VSD deactivation mechanism obtained in silico is consistent with experiments and kinetic models as it proceeds via sequential steps.

The gating charges for each transition estimated from the molecular models ( $\sim 0.45$  to  $1.2e$  per subunit) are of the same order of magnitude as the elementary charge estimated from measurements of gating current fluctuations<sup>35</sup> and as the early component of the gating current recorded in *Shaker* channels ( $\sim 1e$  per VSD unit).<sup>12,36</sup> The mechanism involves in particular specific interactions and a sequential breaking and forming of salt bridges within the VSDs that agrees with early mutagenesis experiments<sup>37</sup> and with more recent experiments probing specific interactions in the intermediate states of the VSDs of VGCCs.<sup>18</sup> Another recent MD simulation study totaling  $>1$  ms simulations has reached similar conclusions, while also providing exciting results about the entire channel opening/closing and VSD-pore coupling mechanism.<sup>38</sup> Finally, electrophysiology recordings of  $\text{Cd}^{2+}$ -bridged double cystein mutants of *Shaker* have enabled to build ab initio models of an active state similar to the crystal structure and four more resting ones,<sup>39</sup> that bear strong similarities to our  $\alpha$ ,  $\beta$ ,  $\gamma$ ,  $\delta$  and  $\epsilon$  states.

In agreement with a recent mutagenesis study,<sup>40</sup> the basic residues of S4 (K5, R4, R3, R2, and R1) were found to occupy the occluded site identified in the VSD of the  $\text{K}^+$  VGCCs (formed by two negatively charged residues (D<sup>259</sup>, E<sup>236</sup> in *Shaker*) and the highly conserved F<sup>233</sup> of S2) in the  $\alpha$ ,  $\beta$ ,  $\gamma$ ,  $\delta$ , and  $\epsilon$  VSD conformations, respectively (Figure 1). Further analyzes of the gating charge transported by each basic residue based on free energy considerations<sup>33,35</sup> showed that the residue translocating through the occluded site during each transition accounts for most of the gating charge, rationalizing the denomination of this site as a "gating charge transfer center".

Hence, today, a large body of evidence suggests that the intermediate states are of functional significance<sup>38,41</sup> while a number of five conformations, as deduced from our work, agrees with the most recent experiments.<sup>39,40</sup> Quite interestingly, we found that the local electric field is focused within the VSD and points downward in all five states, in agreement with fluorescence measurements.<sup>42</sup> Switching from the activated to the deactivated state involves mainly a  $\sim 10$ – $15$  Å downward translation of the S4 residues with respect to the remaining other three static helices, coupled to a significant counter-clockwise helical twisting ( $\sim 90^\circ$ ), consistent with the helical screw model.<sup>13,14</sup> Other simulations have also reported that a change in secondary structure (from an alpha to a  $3_{10}$  helix) of the short stretch of the S4 helix transiting through the gating charge transfer center<sup>39,43</sup> is important for the deactivation mechanism, in agreement with crystallographic and indirect structural data.<sup>44,45</sup> Most

molecular models proposed so far for the resting state Kv1.2, using the ab initio/homology modeling approach and/or voltage-biased MD simulations, have now converged toward similar characteristics. In particular, the location of the backbone atoms is similar in almost all models of the down state.<sup>46</sup> The only discrepancy lies in the position of the side chain of R1, that is placed in interaction with E226 in one type of models<sup>24</sup> while been located close to D283 in the other.<sup>25,39</sup> As authors claim that most experimental constraints are compatible with either of the models,<sup>34,40,47,48</sup> it is likely that both families of conformations are populated at hyperpolarized voltages in proportions that remain to be assessed.

Several other interesting and peculiar properties of VGCCs could be extracted from MD simulations, such as the role lipids play in the activation process. Indeed, the lipid negatively charged phosphate head-groups provide countercharges for the S4 basic residues during the activation process and stabilize thereby not only the activated and the resting state, as shown by others,<sup>23,28,49–52</sup> but also the intermediate ones. This helps to rationalize why the perturbation of the lipid composition embedding the channel deeply alters its function,<sup>53,54</sup> a mode of action which the spider *Loxosceles reclusa* uses to paralyze its prey, its venom containing an enzyme that targets lipid head-groups.<sup>55</sup> With the availability of molecular models of the channel in its lipid environment, we can now address questions that pertain to the modulation of the function of VGCCs by lipids alteration. The following paragraph highlights another type of modulation mechanism and depicts in more details how we used the Kv1.2 VSD conformations to investigate the effect of S4 basic residues mutations at the molecular level.

## S4 Basic Residues Mutations Cause Leak Currents

A large number of diseases result from the dysfunction of VGCCs caused by inherited genetic mutations of their genes.<sup>2</sup> Most channelopathies have dominant inheritance and are caused by mutations that enhance VGCC activation or impair inactivation. Today, the molecular mechanisms that explain defects in ion channel function remain ambiguous. However, several diseases originate from mutations located within the VSDs, and specifically on S4. Because these residues confer the VSD its sensitivity, their mutations modifies the response to voltage changes and alters therefore their function.<sup>56</sup>

Recently however, electrophysiology experiments identified some mutations that prompt the appearance of a current component independent from the canonical alpha conduction. The authors attributed this so-called "omega" or

gating-pore current to a leakage of cations through an unidentified conduction pathway within the VSD. "Artificial" mutants of *Shaker* were first studied: substitution of R1 with histidine, R1H, allows a proton current to flow at hyperpolarized potentials, while a R4H mutant induces a flux at depolarized potentials.<sup>57</sup> Moreover, mutations of R1 into smaller, uncharged residues trigger an influx of a nonselective cation omega current through the VSD at hyperpolarized potentials.<sup>58,59</sup> Further work on *Shaker* revealed that only in the resting state does a single mutation (R1S) trigger the appearance of an omega current. In more activated states, double mutations (R1S and R2S, or R2S and R3S) are required for cation conductance.<sup>60</sup> In Nav1.4, mutations of R2 or R3 to uncharged aminoacids allow a state-dependent influx of cations through the omega pore and are shown to cause periodic paralyses.<sup>61–63</sup> Furthermore, for R1H mutants in Nav1.4 domains I and II and for R2H mutants in domain III, the H<sup>+</sup> omega current appears only when the channel is in its hyperpolarized conformation and the omega pore closes under depolarization.<sup>64</sup>

Sequence and structure similarity between the members of the large family of VGCCs (Nav, Cav and Kv) rationalizes the use of Kv1.2 as a prototype to study the effect of S4 mutations on the stability and conduction properties of such channels. As no Kv1.2 mutant leads to a genetic disease, we have considered various "artificial mutants" and characterized features of the corresponding channel after substitution of specific S4 charges. One of the main characteristics of the Kv channels VSD topology is the presence of large water crevices that penetrate the structure from the intra and extra cellular media, both in the active and in the resting state,<sup>50,51,65,66</sup> as shown by solvent accessibility measurements.<sup>67</sup> The state-dependent salt bridge network formed by S4 positive charges and their counterparts shapes a constriction that prevents communication between the two media (Figure 2).<sup>34</sup> One expects that the mutation of the residues involved in this constriction (bottom ones in the activated and top ones in the resting state) will affect the VSD stability.

We have therefore generated a set of simulations of the Kv1.2 full channel, in the open and the closed state, for which these specific residues were substituted by uncharged equivalents, thereby mimicking their mutation to glutamine.<sup>34</sup> As control simulations, we studied both the wild type and mutants of basic residues not involved in the constriction. All mutations to uncharged residues disrupt the salt bridge in which the residue participates. However, as expected, only the mutation of residues involved in the constriction region (K5/R6 double mutant and K5 single

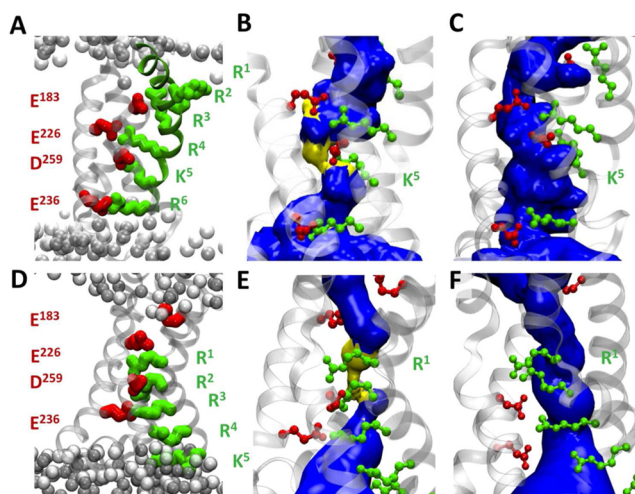


**FIGURE 2.** VSD Topologies of the activated (top panels) and resting (lower panels) Kv1.2 channel conformations. (A and D) Location of the S4 basic residues (green) and the salt bridges they form with acidic charges (red). (B and E) Topology of the solvent-accessible volume (blue) the wild type VSDs. The most constricted regions (pore radius <1.15 Å) are highlighted in yellow. (C and F) K5 and R1 respective mutants, in which omega pores are formed. Copyright 2010 from BJ.

mutant in the activated state and R1 single mutant in the resting one) opens up a hydrophilic pathway connecting the intra- and extracellular media, the omega<sup>1</sup> pore (Figure 2).

We have then submitted all systems to high transmembrane voltages  $\Delta V$  to identify which ones were permeable to ions. In the  $\alpha$  state, a large depolarized voltage induced outward K<sup>+</sup> conduction in the double (K5/R6) mutant. Our activated K5 single mutant, on the other hand, displayed no conduction event over the time scale of the simulation. Note that mutants of these two basic side chains could not yet be examined by experiments so far, due to the lack of expression of K5/R6 mutants. In the  $\epsilon$  state, a large hyperpolarized transmembrane voltage generated inward K<sup>+</sup> conduction in the single R1 mutant. As the number of K<sup>+</sup> permeation events we collected (2 over 40 ns) precludes us from extracting meaningful conductance values, it is interesting to mention the results of two subsequent MD simulation studies reporting for the first time omega current conductance values in agreement with experimental measurements for an R1S mutant in an alternate model of the closed state of Kv1.2<sup>68</sup> and R2S mutant of a Kv1.2/2.1 resting state model.<sup>38</sup> Hence, considering the past<sup>59,61,63</sup> and present results, a pattern emerges (Figure 3):

- At rest, under hyperpolarized transmembrane voltage, S4 is in the "down" state, constraining the VGCC pore in a closed conformation. Within the VSD, the salt bridges that maintain the constriction bridging the intra- and

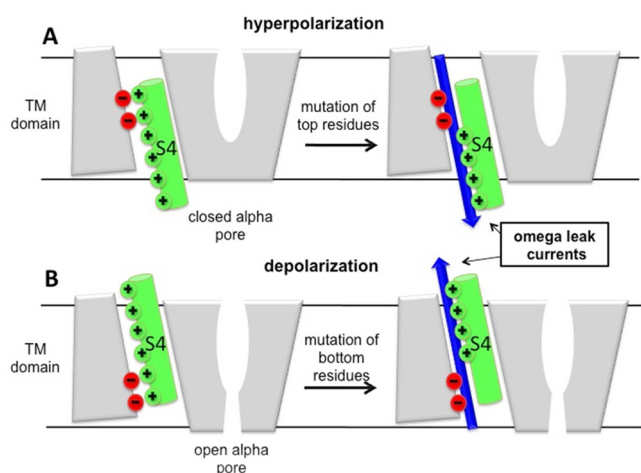


**FIGURE 3.** (A) Under hyperpolarized potentials, the VGCCs are closed. Omega currents represent an inward cation leak (blue arrow). (B) Under depolarized potentials, the channel is open. Omega outward currents are a modulation of the alpha (central pore) current unless the channel inactivates at prolonged depolarized potentials. Copyright 2010 from BJ.

extracellular solution crevices involve the top basic residues of S4. Only their mutation destabilizes the VSD and may lead to omega “leak” currents through a hydrophilic pathway.

- Upon activation, under depolarized transmembrane potentials, S4 positive residues move upward, leading the main pore to open. Within the VSD, bottom S4 basic residues bridge between the two solution crevices and accordingly, their mutation destabilizes the VSDs and may lead to omega currents.

These two scenarios are consistent with experiments where leak currents were recorded under hyperpolarized potentials in Na selective<sup>61,69</sup> and in *Shaker* channels<sup>58</sup> and under depolarized potentials in Na channels.<sup>61,63</sup> They also rationalize their incidence on the channel's molecular function: under hyperpolarized transmembrane potentials, VGCCs are impermeable to ions and omega currents constitute a real leak. Most mutations involved in genetic diseases fall in this category. Under depolarized transmembrane potentials on the other hand, VGCCs are open and the omega currents, estimated experimentally to be ~2 orders of magnitude lower than alpha pore currents, barely modulate the alpha current,<sup>61</sup> except in inactivating channels. Note that such mutants are suspected to have evolved into biologically relevant channels: a flatworm channel in which two S4 basic residues are replaced by neutral ones acts as an inward-rectifier.<sup>70</sup> Comparably, the voltage-gated proton channel only bears three S4 basic residues, enabling proton transport presumably through a VSD pore.<sup>71,72</sup>

As genetic mutations are still identified, modeling studies along these lines will enable one to determine which specific mutation detected in a given channelopathy may yield omega currents. Accurate models of the 3d structure of the channel of interest are required, enabling to characterize the state-dependent VSD salt bridge network. As new VGCCs crystal structures emerge or more precise homology models are built, it becomes possible to identify precisely which residues are critical. Hence, despite the uncertainties that are inherent to homology modeling, robust models of Kv or Nav channels built for instance using as templates the recently determined bacterial sodium channel crystal structures<sup>73</sup> can constitute a good approximation to gain an insight in the effect of genetic mutations of human VGCCs.<sup>64</sup> For completeness, one should also note that the appearance of omega currents is most likely not the only effect of S4 basic residues mutations: recorded shifts in *G/V* and *Q/V* curves and modified kinetics of ON and OFF currents<sup>74</sup> show that such mutations also modulate the VSD response to transmembrane voltage changes, an effect that remains to be investigated by MD simulations.

In summary, molecular modeling enables nowadays to contribute to answer questions of increasing biological relevance. Taken together with data from various experiments and simulations, our results reveal that a consensus on the long debated deactivation mechanism of the VSD of Shaker-like channels is emerging: such a process most likely follows a helical screw pathway while involving five states in Kv1.2 (activated, three intermediate, and resting state), each bearing a specific salt bridge pattern. Availability of such fine structural data now enables, using the approach developed in this contribution as well as state-of-the-art enhanced sampling methods, to tackle questions pertaining to the modulation of VGCCs by mutations, toxins, anesthetics or other mechanisms and will undoubtedly contribute to shed new light onto the molecular level mechanisms involved in these processes.

*We thank Werner Treptow and Michael L. Klein for insightful discussions. This work was performed using HPC resources from GENCI-CINES Grant 2010-2012-075137.*

#### BIOGRAPHICAL INFORMATION

**Mounir Tarek** was born in Rabat-Morocco in 1964. He received a Ph.D. in Physics from the University of Paris in 1994. He is a senior research scientist (Directeur de Recherches) at the CNRS. He joined the CNRS after a four years tenure at the National Institute of Standards and Technology (Gaithersburg, MD) following three

years tenure at the University of Pennsylvania (Postdoc in the M. L. Klein group). For the past few years, he has worked on large-scale molecular simulations of lipid membranes and transmembrane proteins, probing their structure and dynamics.

**Lucie Delemotte** was born in France in 1985. She received her M.Sc. from the University of Nancy, France in 2008. Recipient of the Ph.D. in 2011 from the University of Nancy, she was awarded a Marie Curie IOF fellowship from the European commission to work as a postdoctoral fellow in the Klein Group at Temple University, Philadelphia, PA. She is interested in unraveling the function of ion channels using a combination of state-of-the-art computational methods.

## FOOTNOTES

\*To whom correspondence should be addressed. Mailing address: UMR 7565 – SRSMC, Faculté des Sciences et Techniques, B.P. 70239, 54506 Vandoeuvre les Nancy, Université de Lorraine, France. Tel: +33 (0)3 83 68 43 74. E-mail: Mounir.Tarek@univ-lorraine.fr. The authors declare no competing financial interest.

<sup>†</sup>L.D.: Institute for Computational Molecular Science, Temple University, Philadelphia, PA, USA.

## REFERENCES

- Hille, B. *Ion channels of excitable membranes*, 3rd ed.; Sinauer Associates Inc.: Sunderland, MA, 2001.
- Lehmann-Horn, F.; Jurkat-Rott, K. Voltage-gated ion channels and hereditary disease. *Physiol. Rev.* **1999**, *79*, 1517.
- Armstrong, C. M.; Bezanilla, F. Inactivation of the sodium channel. II. Gating current experiments. *J. Gen. Physiol.* **1977**, *70*, 567–590.
- Seoh, S. A.; Sigg, D.; Papazian, D. M.; Bezanilla, F. Voltage-sensing residues in the S2 and S4 segments of the Shaker K<sup>+</sup> channel. *Neuron* **1996**, *16*, 1159–1167.
- Aggarwal, S. K.; MacKinnon, R. Contribution of the S4 segment to gating charge in the Shaker K<sup>+</sup> channel. *Neuron* **1996**, *16*, 1169–1177.
- Zagotta, W. N.; Hoshi, T.; Aldrich, R. W. Shaker potassium channel gating. III: Evaluation of kinetic models for activation. *J. Gen. Physiol.* **1994**, *103*, 321.
- Schoppa, N. E.; Sigworth, F. J. Activation of Shaker potassium channels. III. An activation gating model for wild-type and V2 mutant channel. *J. Gen. Physiol.* **1998**, *111*, 313–342.
- Gagnon, D. G.; Bezanilla, F. A single charged voltage sensor is capable of gating the Shaker K<sup>+</sup> channel. *J. Gen. Physiol.* **2009**, *133*, 467–483.
- Baker, O.; Larsson, H.; Mannuzzo, L.; Isacoff, E. Three transmembrane conformations and sequence-dependent displacement of the S4 domain in Shaker K channel gating. *Neuron* **1998**, *20*, 1283–1294.
- Kanevsky, M.; Aldrich, R. W. Determinants of voltage-dependent gating and open-state stability in the S5 segment of Shaker potassium channels. *J. Gen. Physiol.* **1999**, *114*, 215–242.
- Loboda, A.; Armstrong, C. M. Resolving the gating charge movement associated with late transitions in K channel activation. *Biophys. J.* **2001**, *81*, 905–916.
- Sigg, D.; Bezanilla, F.; Stefani, E. Fast gating in the shaker K<sup>+</sup> channel and the energy landscape of activation. *Proc. Natl. Acad. Sci. U.S.A.* **2003**, *100*, 7611–7615.
- Guy, H. R.; Seetharamulu, P. Molecular model of the action potential sodium channel. *Proc. Natl. Acad. Sci. U.S.A.* **1986**, *83*, 508–512.
- Catterall, W. A. Voltage-dependent gating of sodium channels: correlating structure and function. *Trends Neurosci.* **1986**, *9*, 7–20.
- Tiwari-Woodruff, S. K.; Lin, M. A.; Schulteis, C. T.; Papazian, D. M. Voltage-dependent structural interactions in the Shaker K<sup>+</sup> channel. *J. Gen. Physiol.* **2000**, *115*, 123.
- Bezanilla, F. The voltage sensor in voltage-dependent ion channels. *Physiol. Rev.* **2000**, *80*, 555–592.
- Jiang, Y.; Ruta, V.; Chen, J.; Lee, A.; MacKinnon, R. The principle of gating charge movement in a voltage-dependent K<sup>+</sup> channel. *Nature* **2003**, *423*, 42–48.
- Catterall, W. A. Ion channel voltage sensors: Structure, function, and pathophysiology. *Neuron* **2010**, *67*, 915–928.
- Long, B. S.; Campbell, E. B.; MacKinnon, R. Crystal structure of a mammalian voltage-dependent Shaker family K<sup>+</sup> channel. *Science* **2005**, *309*, 897–903.
- Durell, S. R.; Shrivastava, I. H.; Guy, H. R. Models of the structure and voltage-gating mechanism of the shaker K<sup>+</sup> channel. *Biophys. J.* **2004**, *87*, 2116–2130.
- Yarov-Yarovoy, V.; Baker, D.; Catterall, W. A. Voltage sensor conformations in the open and closed states in Rosetta structural models of K<sup>+</sup> channels. *Proc. Natl. Acad. Sci. U.S.A.* **2006**, *103*, 7292–7297.
- Pathak, M. M.; Yarov-Yarovoy, V.; Agarwal, G.; Roux, B.; Barth, P.; Kohout, S.; Tombola, F.; Isacoff, E. Y. Closing in on the resting state of the shaker K<sup>+</sup> channel. *Neuron* **2007**, *56*, 124–140.
- Khalili-Araghi, F.; Jogini, V.; Yarov-Yarovoy, V.; Tajkhorshid, E.; Roux, B.; Schulten, K. Calculation of the gating charge for the Kv1.2 voltage activated potassium channel. *Biophys. J.* **2010**, *98*, 1–10.
- Vargas, E.; Bezanilla, F.; Roux, B. In search of a consensus model of the resting state of a voltage-sensing domain. *Neuron* **2011**, *72*, 713–720.
- Delemotte, L.; Tarek, M.; Klein, M. L.; Amaral, C.; Treptow, W. Intermediate states of the Kv1.2 voltage sensor from atomistic molecular dynamics simulations. *Proc. Acad. Natl. Sci. U.S.A.* **2011**, *108*, 6109–6114.
- Treptow, W.; Maigret, B.; Chipot, C.; Tarek, M. Coupled motions between pore and voltage-sensor domains: a model for Shaker B, a voltage-gated potassium channel. *Biophys. J.* **2004**, *87*, 2365–2379.
- Nishizawa, M.; Nishizawa, K. Molecular dynamics simulation of Kv channel voltage sensor helix in a lipid membrane with applied electric field. *Biophys. J.* **2008**, *95*, 1729–1744.
- Bjelkmar, P.; Niemelä, P. S.; Vattulainen, I.; Lindahl, E. Conformational changes and slow dynamics through microsecond polarized atomistic molecular simulation of an integral Kv1.2 ion channel. *PLoS Comput. Biol.* **2009**, *5*, e1000289.
- Roux, B. The membrane potential and its representation by a constant electric field in computer simulations. *Biophys. J.* **2008**, *95*, 4205–4216.
- Delemotte, L.; Tarek, M. Molecular dynamics simulations of voltage-gated cation channels: insights on voltage-sensor domain function and modulation. *Front. Pharmacol.* **2012**, *3*, 97.
- Delemotte, L.; Dehez, F.; Treptow, W.; Tarek, M. Modeling membranes under a transmembrane potential. *J. Phys. Chem. B* **2008**, *112*, 5547–5550.
- Denning, E. J.; Crozier, P. S.; Sachs, J. N.; Woolf, T. B. From the gating charge response to pore domain movement: Initial motions of Kv1.2 dynamics under physiological voltage changes. *Mol. Membr. Biol.* **2009**, *26*, 397–421.
- Treptow, W.; Tarek, M.; Klein, M. L. Initial response of the potassium channel voltage sensor to a transmembrane potential. *J. Am. Chem. Soc.* **2009**, *131*, 2107–2110.
- Delemotte, L.; Treptow, W.; Klein, M. L.; Tarek, M. Effect of sensor domain mutations on the properties of voltage-gated ion channels: Molecular dynamics studies of the channel Kv1.2. *Biophys. J.* **2010**, *99*, L72–L74.
- Sigworth, F. J. Voltage gating of ion channels. *Q. Rev. Biophys.* **1994**, *27*, 1–40.
- Freites, J. A.; Schow, E. V.; White, S. H.; Tobias, D. J. Microscopic origin of gating current fluctuations in a potassium channel voltage-sensor. *Biophys. J.* **2012**, *102*, A44–A46.
- Papazian, D. M.; Shao, X. M.; Seoh, S.; Mock, A. F.; Huang, Y.; Wainstock, D. H. Electrostatic interactions of S4 voltage sensor in Shaker K<sup>+</sup> channel. *Neuron* **1995**, *14*, 1293–1301.
- Jensen, M. O.; Jogini, V.; Borhani, D. W.; Leffler, A. E.; Dror, R. O.; Shaw, D. E. Mechanism of voltage gating in potassium channels. *Science* **2012**, *336*, 229–233.
- Henrion, U.; Renhorn, J.; Borjesson, S. I.; Nelson, E. M.; Schwaiger, C. S.; Bjelkmar, P.; Wallner, B.; Lindahl, E.; Elinder, F. Tracking a complete voltage sensor cycle with metal-ion bridges. *Proc. Natl. Acad. Sci. U.S.A.* **2012**, *109*, 8552–8557.
- Tao, X.; Lee, A.; Limapichat, W.; Dougherty, D. A.; MacKinnon, R. A gating charge transfer center in voltage sensors. *Science* **2010**, *328*, 67–73.
- DeCaen, P. G.; Yarov-Yarovoy, V.; Sharp, E. M.; Scheuer, T.; Catterall, W. A. Sequential formation of ion pairs during activation of a sodium channel voltage sensor. *Proc. Natl. Acad. Sci. U.S.A.* **2009**, *106*, 22498.
- Asamoah, O. K.; Wuskell, J. P.; Loew, L. M.; Bezanilla, F. A fluorometric approach to local electric field measurements in a voltage-gated ion channel. *Neuron* **2003**, *37*, 85–97.
- Schwaiger, C. S.; Bjelkmar, P.; Hess, B.; Lindahl, E. 310-helix conformation facilitates the transition of a voltage sensor S4 segment toward the down state. *Biophys. J.* **2011**, *100*, 1446–1454.
- Clayton, G. M.; Altieri, S.; Heginbotham, L.; Unger, V. M.; Morais-Cabral, J. H. Structure of the transmembrane regions of a bacterial cyclic nucleotide-regulated channel. *Proc. Natl. Acad. Sci. U.S.A.* **2008**, *105*, 15111–15115.
- Villalba-Galea, C. A.; Sandtner, W.; Starace, D. M.; Bezanilla, F. S4-based voltage sensors have three major conformations. *Proc. Natl. Acad. Sci. U.S.A.* **2008**, *105*, 17600.
- Vargas, E.; Yarov-Yarovoy, V.; Khalili-Araghi, F.; Catterall, W. A.; Klein, M. L.; Tarek, M.; Lindahl, E.; Schulten, K.; Perozo, E.; Bezanilla, F.; Roux, B. An emerging consensus on voltage-dependent gating from computational modeling and molecular dynamics simulations. *J. Gen. Physiol.* **2012**, *140*, 587–594.
- Campos, F. V.; Chanda, B.; Roux, B.; Bezanilla, F. Two atomic constraints unambiguously position the S4 segment relative to S1 and S2 segments in the closed state of Shaker K channel. *Proc. Natl. Acad. Sci. U.S.A.* **2007**, *104*, 7904–7909.
- Lin, M. A.; Hsieh, J.-Y.; Mock, A. F.; Papazian, D. M. R1 in the Shaker S4 occupies the gating charge transfer center in the resting state. *J. Gen. Physiol.* **2011**, *138*, 155–163.
- Freites, J. A.; Tobias, D. J.; Von Heijne, G.; White, S. H. Interface connections of a transmembrane voltage sensor. *Proc. Natl. Acad. Sci. U.S.A.* **2005**, *102*, 15059–15064.

- 50 Treptow, W.; Tarek, M. Environment of the gating charges in the Kv1.2 Shaker potassium channel. *Biophys. J.* **2006**, *90*, L64–L66.
- 51 Jogini, V.; Roux, B. Dynamics of the Kv1.2 voltage-gated K<sup>+</sup> channel in a membrane environment. *Biophys. J.* **2007**, *93*, 3070–3082.
- 52 Sands, Z. A.; Sansom, M. S. P. How does a voltage sensor interact with a lipid bilayer? Simulations of a potassium channel domain. *Structure* **2007**, *15*, 235–244.
- 53 Schmidt, D.; Jiang, Q.; MacKinnon, R. Phospholipids and the origin of cationic gating charges in voltage sensors. *Nature* **2006**, *444*, 775–779.
- 54 Abderemane-Ali, F.; Es-Salah-Lamoureux, Z.; Delemotte, L.; Kasimova, M. A.; Labro, A. J.; Snyders, D. J.; Fedida, D.; Tarek, M.; Baro, I.; Loussouarn, G. Dual effect of PIP<sub>2</sub> on Shaker potassium channels. *J. Biol. Chem.* **2012**, *287*, 36158–36167.
- 55 Xu, Y.; Ramu, Y.; Lu, Z. Removal of phospho-head groups of membrane lipids immobilizes voltage sensors of K<sup>+</sup> channels. *Nature* **2008**, *451*, 826–829.
- 56 Bao, H.; Hakeem, A.; Henteleff, M.; Starkus, J. G.; Rayner, M. D. Voltage-insensitive gating after charge-neutralizing mutations in the S4 segment of shaker channels. *J. Gen. Physiol.* **1999**, *113*, 139–151.
- 57 Starace, D. M.; Bezanilla, F. Histidine scanning mutagenesis of basic residues of the S4 segment of the shaker potassium channel. *J. Gen. Physiol.* **2001**, *117*, 469–490.
- 58 Tombola, F.; Pathak, M. M.; Isacoff, E. Y. Voltage-sensing arginines in a potassium channel permeate and occlude cation-selective pores. *Neuron* **2005**, *45*, 379–388.
- 59 Tombola, F.; Pathak, M. M.; Gorostiza, P.; Isacoff, E. Y. The twisted ion-permeation pathway of a resting voltage-sensing domain. *Nature* **2006**, *445*, 546–549.
- 60 Gamal El-Din, T. M.; Heldstab, H.; Lehmann, C.; Greeff, N. G. Double gaps along Shaker S4 demonstrate omega currents at three different closed states. *Channels* **2010**, *4*, 93–100.
- 61 Sokolov, S.; Scheuer, T.; Catterall, W. A. Ion permeation through a voltage-sensitive gating pore in brain sodium channels having voltage sensor mutations. *Neuron* **2005**, *47*, 183–189.
- 62 Struyk, A. F.; Cannon, S. C. A Na<sup>+</sup> channel mutation linked to hypokalemic periodic paralysis exposes a proton selective gating pore. *J. Gen. Physiol.* **2007**, *130*, 11–20.
- 63 Sokolov, S.; Scheuer, T.; Catterall, W. A. Depolarization-activated gating pore current conducted by mutant sodium channels in potassium-sensitive normokalemic periodic paralysis. *Proc. Natl. Acad. Sci. U.S.A.* **2008**, *105*, 19980–19985.
- 64 Gosselin-Badaroudine, P.; Delemotte, L.; Moreau, A.; Klein, M. L.; Chahine, M. Gating pore currents and the resting state of Nav1.4 voltage sensor domains. *Proc. Natl. Acad. Sci. U.S.A.* **2012**, *109*, 19250–19255.
- 65 Freites, J. A.; Tobias, D. J.; White, S. H. A voltage-sensor water pore. *Biophys. J.* **2006**, *91*, L90–L92.
- 66 Krepkij, D.; Mihailescu, M.; Freites, J. A.; Schow, E. V.; Worcester, D. L.; Gawrisch, K.; Tobias, D. J.; White, S. H.; Swartz, K. J. Structure and hydration of membranes embedded with voltage-sensing domains. *Nature* **2009**, *462*, 473–479.
- 67 Larsson, H. P.; Baker, O. S.; Dhillon, D. S.; Isacoff, E. Y. Transmembrane movement of the Shaker K<sup>+</sup> Channel S4. *Neuron* **1996**, *16*, 387–397.
- 68 Khalili-Araghi, F.; Tajkhorshid, E.; Roux, B.; Schulten, K. Molecular dynamics investigation of the ω-current in the Kv1.2 voltage sensor domains. *Biophys. J.* **2012**, *102*, 258–267.
- 69 Gosselin-Badaroudine, P.; Keller, D. I.; Huang, H.; Pouliot, V.; Chatelier, A.; Osswald, S.; Brink, M.; Chahine, M. A proton leak current through the cardiac sodium channel is linked to mixed arrhythmia and the dilated cardiomyopathy phenotype. *PLoS One* **2012**, *7*, e38331.
- 70 Klassen, T. L.; Spencer, A. N.; Gallin, W. J. A naturally occurring omega current in a Kv3 family potassium channel from a platyhelminth. *BMC Neurosci.* **2008**, *9*, 52–64.
- 71 Ramsey, I. S.; Mokrab, Y.; Carvacho, I.; Sands, Z. A.; Sansom, M. S. P.; Clapham, D. E. An aqueous H<sup>+</sup> permeation pathway in the voltage-gated proton channel Hv1. *Nat. Struct. Mol. Biol.* **2010**, *17*, 869–875.
- 72 Wood, M. L.; Schow, E. V.; Freites, J. A.; White, S. H.; Tombola, F.; Tobias, D. J. Water wires in atomistic models of the Hv1 proton channel. *Biochim. Biophys. Acta* **2012**, *1818*, 286–293.
- 73 Payandeh, J.; Scheuer, T.; Zheng, N.; Catterall, W. A. The crystal structure of a voltage-gated sodium channel. *Nature* **2011**, *475*, 353–358.
- 74 Miceli, F.; Soldovieri, M. V.; Hernandez, C. C.; Shapiro, M. S.; Annunziato, L.; Tagliatalata, M. Gating consequences of charge neutralization of arginine residues in the S4 segment of Kv7.2, an epilepsy-linked K<sup>+</sup> channel subunit. *Biophys. J.* **2008**, *95*, 2254–2264.